Planar Circuit Analysis of Microstrip Radial Stub

FRANCO GIANNINI, MEMBER, IEEE, ROBERT SORRENTINO, MEMBER, IEEE, AND JAN VRBA

Abstract — **Radial-line stubs have been found to work better than low-impedance rectangular stubs when an accurate localization of a zero-point impedance is needed. In this paper, microstrip radial-line stubs are analyzed using a planar circuit technique and characterized for design purposes. Experiments performed on various structures are in excellent agreement with the theory and confirm the suitability of such a structure as an alternative to a conventional straight stub.**

I. Introduction

A NUMBER of microstrip circuits, such as low-pass filters, bias filter elements, mixers, etc., often require the use of shunt stubs with characteristic impedance as low as 10–20 Ω. At high frequencies, however, a microstrip line section with such a low characteristic impedance has a width which is a significant fraction of the wavelength; higher order modes can be easily excited and the structure behavior differs significantly from that predicted on the basis of a one-dimensional transmission-line model. Moreover, the large width of the stub renders its location poorly defined. In order to overcome these problems, the use of radial-line stubs has been suggested [1].

In particular, Vinding [1] has proposed a formula for evaluating the input reactance of microstrip radial stubs. Based on Vinding's formula, Atwater [2] has recently developed a design procedure of radial stubs. Like other formulas for microstrip planar circuits which are based on a mere magnetic wall model, however, Vinding's formula does not yield sufficiently accurate results.

A planar circuit analysis of a microstrip radial stub is presented in this paper. The method is based on the electromagnetic (EM) field expansion in terms of resonant modes of the planar structure [3] and has been successfully applied to other similar problems [4].

II. Electromagnetic Model

The EM-field expansion in terms of resonant modes in a planar circuit has already been applied to rectangular, circular [3], and annular structures [4].

As shown in [3], accurate results can be obtained through a magnetic wall model, provided effective dimensions and effective permittivities properly defined for each resonant mode are used. Moreover, it is worth specifying that different effective parameters should be used depending on the type of connection of the stub to the external circuit. For instance, as sketched in Fig. 1, account has also to be taken of the effective width of the feeding line, so that different effective geometries result when the stub terminates a line section (Fig. 1(a)) or is shunt connected (Fig. 1(b)). In any case, assuming that the effective width of the input port of the planar stub is much smaller than the wavelength, only TM_{on} mode ($n = 0,1,2,\cdots$) resonant modes will be excited. Therefore, the effective dimensions and effective permittivities can be easily obtained following the same procedure as in [5] and [6], and on the basis of the following assumptions.

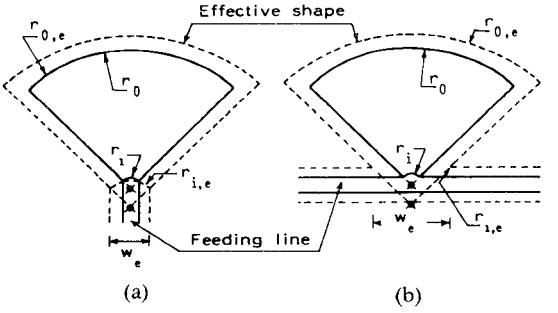

Fig. 1. Geometries of (a) series and (b) shunt connected radial stubs.

a) The effective angle is equal to the actual angle α.

b) The end effect at the external edge of the structure is the same as in a circular structure.

c) The effective width w_e of the input port is the same as that of a uniform microstrip line of width w. It can be computed using well-known formulas [7].

One obtains

$$r_{ie} = \frac{w_e}{2\sin(\alpha/2)} \tag{1}$$

$$r_{oe} = r_o\left\{1 + \frac{2h}{\pi r_o}\left[\ln\left(\frac{\pi r_o}{2h}\right) + 1.7726\right]\right\}^{1/2} + \frac{w_e - w}{2}\begin{cases} \dfrac{1}{\sin(\alpha/2)}, & \text{for } \alpha < \pi \\ 1, & \text{for } \pi < \alpha < 3\pi/2 \end{cases} \tag{2}$$

where h is the dielectric substrate thickness, and w and w_e are the actual and effective widths of the feeding line. The other geometrical parameters are defined in Fig. 1, where the actual geometry together with the effective dimensions

Manuscript received May 8, 1984.

F. Giannini is with the University of Rome, Tor Vergata, Department of Electronic Engineering, 00173 Rome, Italy.

R. Sorrentino is with the University of Rome, La Sapienza, Department of Electronics, 00184 Rome, Italy.

J. Vrba is with the Czech Technical University, 16637 Praha 6, Czechoslovakia.

0018-9480/84/1200-1652$01.00 ©1984 IEEE

of the radial stub are shown. For $\alpha \to 0$, the effective geometry of the radial stub approaches that of a usual straight stub.

It is worth specifying that the present model, which assumes the excitation of TM_{on} modes only, has an upper α limit of applicability, which depends on the type of connection of the stub. In the case of the end termination, the model is not valid when α is such that the radii of the sector are very close to the feeding line; because of the proximity of the radial stub sides to the feeding line, modes other than TM_{on} can be excited and a more complicated model should be adopted.

With regard to the shunt connection, the applicability of the model is restricted to lower values of α. This is not only due to physical reasons ($\alpha < \pi$) but also because of the following arguments. First, in the shunt connection, the EM-field propagating on the feeding line is not truly uniform along the width of the input port; secondly, for a given radial stub, the effective width of the port is larger in the shunt connection than in the end connection, as illustrated in Fig. 1.

On the other hand, the use of a very narrow input port can extend the range of applicability of the present simplified theory in the case of the shunt connection.

With regard to the dynamic effective permittivity of the TM_{on} modes, the expressions quoted in [5] have been used.

The normalized input impedance evaluated at the inner radius r_i in terms of TM_{on} resonant modes is given by

$$Z_{in} = -j\frac{k_g P_{oo}^2}{k^2 \epsilon_{do}} + jk_g \sum_{n=1}^{\infty} \frac{P_{on}^2}{k_{on}^2 - k^2 \epsilon_{dn}} \tag{3}$$

where k_g is the wavenumber of the feeding line, $k = \omega\sqrt{\epsilon_0 \mu_0}$ is the free-space wavenumber, and ϵ_{dn} and k_{on} are the dynamic effective permittivity [5] and the eigenvalue of the TM_{on} mode [3], [4], respectively. P_{on} is the coupling coefficient between the quasi-TEM mode traveling on the feeding line and the TM_{on} mode excited in the stub

$$P_{on} = \sqrt{\frac{w_e}{\pi}} \left[A_{on} J_0(k_{on} r_{ie}) + B_{on} N_0(k_{on} r_{ie})\right] \tag{4}$$

$$A_{on} = \frac{2}{\alpha\pi}\left\{ r_{oe}^2 \left[J_0(k_{on} r_{oe}) + K_n N_0(k_{on} r_{oe})\right]^2 - r_{ie}^2 \left[J_0(k_{on} r_{ie}) + K_n N_0(k_{on} r_{ie})\right]^2 \right\}^{-1} \tag{5}$$

$$B_{on} = K_n A_{on};\ K_n = -J_1(k_{on} r_{oe})/N_1(k_{on} r_{oe}) \tag{6}$$

where J_0 and J_1 are the Bessel functions of the first kind of order 0 and 1; N_0 and N_1 are the Bessel functions of the second kind (Neuman functions) of order 0 and 1.

III. Results

The present theory has been tested on the experiments by Atwater [3], performed on two radial stubs fabricated on a 25-mil alumina substrate, both having an outer radius $r_o = 5.49$ mm [8]. Fig. 2(a) and (b) shows the comparison between the experiments by Atwater and the reactances calculated according to the present theory and by Vinding's formula. Only the first four modes have been used in the expansion. In spite of the low number of modes, the present theory fits the experiments much better than Vinding's formula.

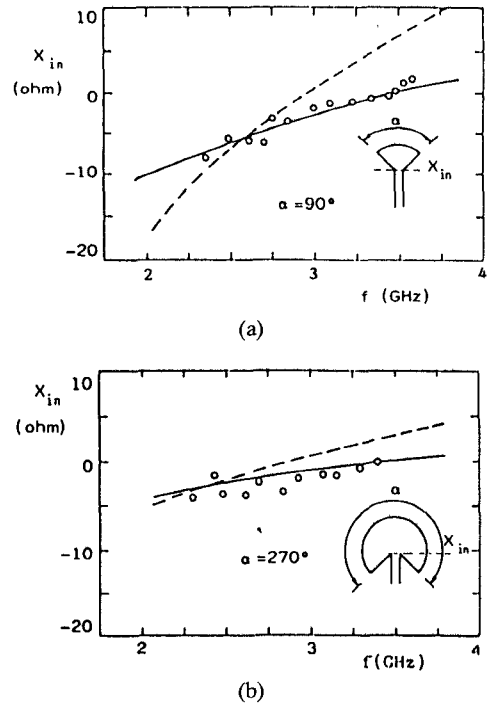

Fig. 2. Input reactance of radial stubs on 0.025-in alumina with (a) sectoral angle $\alpha = 90°$ and (b) sectoral angle $\alpha = 270°$. (——) Present theory, (----) Vinding's formula, (O) experiments after Atwater [2].

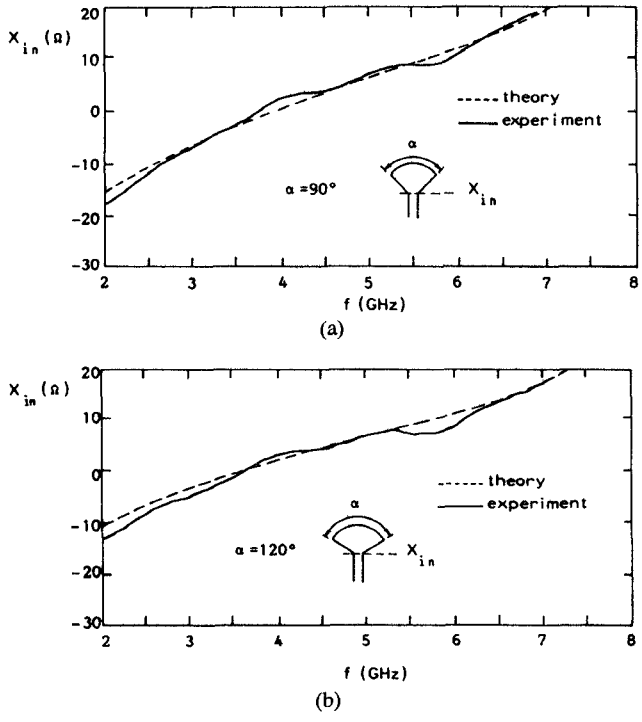

Fig. 3. Frequency behavior of the input reactance of radial stubs with $r_o - r_i = 0.47$ cm; (a) sectoral angle $\alpha = 90°$ and (b) sectoral angle $\alpha = 120°$. Measurements performed on a HP vector analyzer.

Further experiments were performed on radial stubs of 90° and 120° fabricated on the same substrate as in Atwater's experiments. As shown in Fig. 3(a) and (b), a

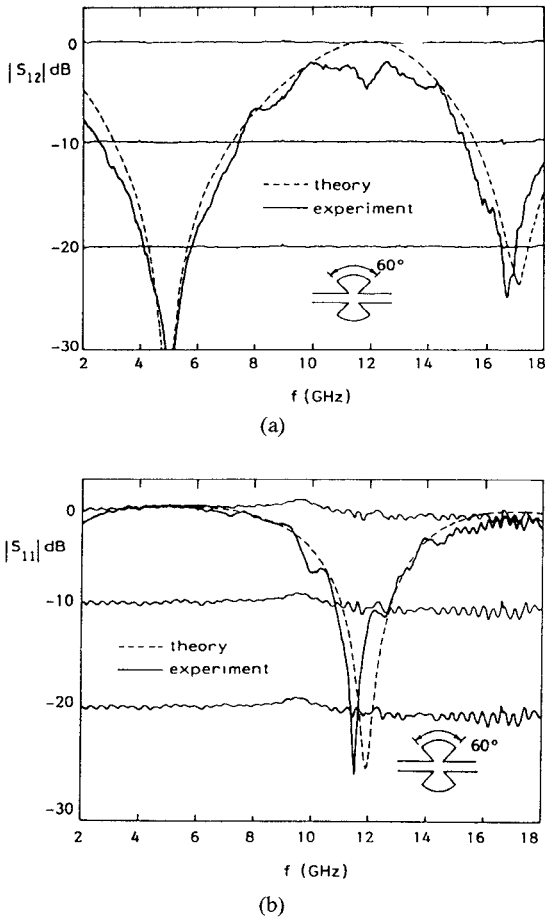

Fig. 4. Frequency behavior of scattering parameters (a) $|S_{12}|$ and (b) $|S_{11}|$ for a "butterfly" stub realized on a 0.0635-cm-thick alumina substrate; $r_o = 0.5$ cm.

very good agreement has been obtained between the theory and the measurements performed on an HP vector network analyzer.

Experiments on shunt stubs were also performed. This is illustrated in Fig. 4, where the scattering parameters $|S_{12}|$, $|S_{11}|$ of a "butterfly" stub, consisting of two 60° shunt stubs with $r_o = 0.5$ cm, are shown in the frequency range 2–18 GHz. The agreement between theory and experiments is highly satisfactory in the whole frequency range.

For design purposes, the radial stub can be usefully characterized in terms of the frequency of zero input reactance f_0 and its equivalent characteristic impedance $Z_0 = (2f_0/\pi)\, dX/df$. The latter quantity is defined as the characteristic impedance of a conventional stub having the same slope parameter at $f = f_0$. Fig. 5(a) and (b) shows the computed behavior of f_0 and Z_0 versus α for microstrip radial stubs with different $r_o - r_i$, series-connected to a 50-Ω feeding line. Experiments performed on radial stubs with $r_o - r_i = 0.47$ cm are in excellent agreement with the theory. Equivalent characteristic impedances as low as 10–15 Ω can be easily obtained with angles α of the order of 120° and $r_o - r_i$ of about 0.5 cm. This figure demonstrates the suitability of a radial-line stub as an alternative to conventional stubs when very low characteristic impedances are required, as suggested by Vinding.

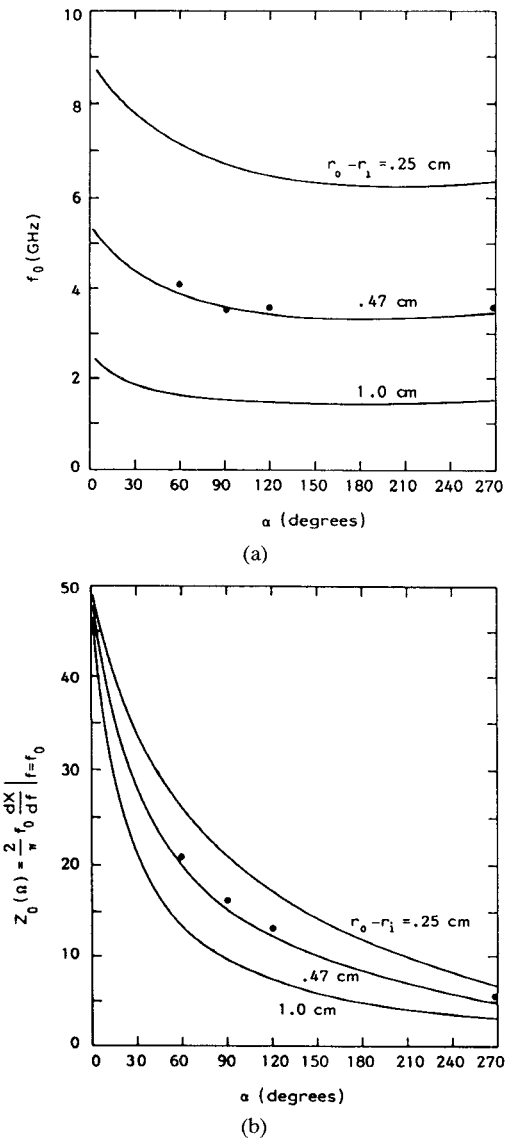

Fig. 5. (a) Frequency of the zero input impedance and (b) equivalent characteristic impedance versus sectoral angle α, for series-connected radial stub.

Finally, the theoretical results of Fig. 6 show that the radial stub can maintain a low-impedance value in a wider frequency range than a conventional straight stub. The input impedance of a 120° radial stub and of a conventional stub with the same slope parameter are plotted versus the normalized frequency f/f_0. The radial stub has an input impedance lower than 20 Ω up to 2 f_0; at this frequency, the conventional stub has an infinite input impedance. Within the approximation used in this short paper, the frequency of infinite reactance of the radial stub is only slightly dependent on the sectoral angle α and close to that of a straight stub $r_o - r_i$ long. Increasing the sectoral angle α, the zero reactance frequency f_0 decreases, thus producing wider low-impedance frequency bands.

II. Conclusions

A planar circuit approach based on the field expansion in terms of resonant modes has been used to characterize a radial-line stub. Measurements of the input impedance as

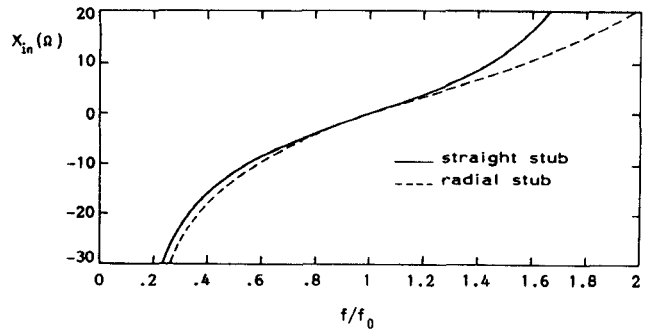

Fig. 6. Computed behaviors of input reactance of a radial stub with $\alpha = 120°$ (----) and a straight stub (——) having the same slope parameter and the same frequency f_0.

well as of the scattering parameters of shunt stubs are in very good agreement with theoretical results. The characterization of the radial stub in terms of an equivalent characteristic impedance has shown the suitability of such a structure as an alternative to the conventional straight stub, as it exhibits a very low characteristic impedance and allows an accurate localization of the impedance reference plane.

ACKNOWLEDGMENT

Prof. T. Itoh is acknowledged for helpful discussions and suggestions.

REFERENCES

[1] J. P. Vinding, "Radial line stubs as elements in strip line circuits," in *NEREM Record*, 1967, pp. 108–109.
[2] A. H. Atwater, "Microstrip reactive circuit elements," *IEEE Trans. Microwave Theory Tech.*, vol. MTT-31, pp. 488–491, June 1983.
[3] G. D'Inzeo, F. Giannini, C. M. Sodi, and R. Sorrentino, "Method of analysis and filtering properties of microwave planar networks," *IEEE Trans. Microwave Theory Tech.*, vol. MTT-26, pp. 462–471, July 1978.
[4] G. D'Inzeo, F. Giannini, R. Sorrentino, and J. Vrba, "Microwave planar networks: The annular structure," *Electron. Lett.*, vol. 14, no. 16, pp. 526–528, Aug. 1978.
[5] J. Vrba, "Dynamic permittivities of microstrip ring resonators," *Electron. Lett.*, vol. 15, no. 16, pp. 504–505, Aug. 1979.
[6] I. Wolff and N. Knoppik, "Rectangular and circular microstrip disk capacitors and resonators," *IEEE Trans. Microwave Theory Tech.*, vol. MTT-22, pp. 857–864, Oct. 1974.
[7] K. C. Gupta, Ramesh Garg, and I. J. Bahl, *Microstrip Lines and Slotlines*. Dedham: Artech House, 1979, chap. 2.
[8] A. H. Atwater, private communication.

Broad-Band Millimeter-Wave *E*-Plane Bandpass Filters

L. Q. BUI, D. BALL, MEMBER, IEEE, AND T. ITOH, FELLOW, IEEE

Abstract—**An accurate method to obtain starting estimates for an *E*-plane bandpass filter CAD program recently developed by Shih, Itoh, and Bui is presented. Results agree very well with exact values for filter design with relative bandwidths exceeding 10 percent at *W*-band and *D*-band and 20 percent at lower frequencies.**

I. INTRODUCTION

WITH INCREASING activity in millimeter-wave integrated circuit development, the *E*-plane filter shown in Fig. 1 recently has drawn considerable attention [1]–[5]. Such a structure consists of metal strips inserted along the *E*-plane of a rectangular waveguide. The strips may be fabricated on dielectric substrates [3]–[5], in which case this filter is quite compatible with finline technology.

To date, many *E*-plane filter designs reported are limited to narrow bandwidths of less than a few percent. For wide-band designs, as all the resonators are strongly coupled, an accurate analysis procedure, one which takes into account the interaction not only of the dominant mode but also of the higher order modes generated at the edge of the strips, is necessary.

We recently developed a computerized (CAD) algorithm for a class of *E*-plane filters [6]. For narrow-band designs, the algorithm converges rapidly with the prescribed response by use of available optimization routines [7]. However, since no systematic scheme was incorporated for providing starting values of the optimization routine, convergence of the CAD program was rather slow; furthermore, the cost of generating acceptable design parameters often was prohibitively expensive. This deficiency is especially noticeable in design of relative bandwidth greater than 5 percent. Since *E*-plane filters are inductively direct-coupled cavity filters, the conventional design procedure given by Levy using an impedance inverter and low-pass prototypes is available as [8]. Depending on the bandwidth equipment, either a lumped-element or a distributed prototype is used to calculate the inverter values. In general, a distributed prototype is not favorable due to difficulties in

Manuscript received April 26, 1984; revised August 1, 1984.

L. Q. Bui and D. Ball are with the Hughes Aircraft Company, Microwave Products Division, Torrence, CA 90509.

T. Itoh is with the Department of Electrical Engineering, the University of Texas at Austin, Austin, TX 78712.

0018-9480/84/1200-1655$01.00 ©1984 IEEE